Biomaterials 31 (2010) 8350–8361

Contents lists available at ScienceDirect

Biomaterials

journal homepage: www.elsevier.com/locate/biomaterials

The kinetics of the tissue distribution of silver nanoparticles of different sizes

D.P.K. Lankveld [a], A.G. Oomen [b], P. Krystek [c], A. Neigh [d], A. Troost – de Jong [c], C.W. Noorlander [b], J.C.H. Van Eijkeren [f], R.E. Geertsma [e], W.H. De Jong [a,*]

[a] Laboratory for Health Protection Research, National Institute for Public Health and the Environment (RIVM), P.O. Box 1, 3720 BA Bilthoven, The Netherlands
[b] Centre for Substances and Integrated Risk Assessment, RIVM, Bilthoven, The Netherlands
[c] MiPlaza Material Analysis, Philips Research Europe, High Tech Campus 12, 5656AE Eindhoven, The Netherlands
[d] NanoComposix 4878 Ronson Ct, San Diego, CA 92111, USA
[e] Centre for Biological Medicines and Medical Technology, RIVM, Bilthoven, The Netherlands
[f] Expertise Centre for Methodology and Information Services, RIVM, Bilthoven, The Netherlands

ARTICLE INFO

Article history:
Received 15 June 2010
Accepted 8 July 2010
Available online 4 August 2010

Keywords:
Silver
Nanoparticles
Tissue distribution
Kinetics

ABSTRACT

Blood kinetics and tissue distribution of 20, 80 and 110 nm silver nanoparticles were investigated in rats up to 16 days after intravenous administration once daily for 5 consecutive days. Following both single and repeated injection, silver nanoparticles disappeared rapidly from the blood and distributed to all organs evaluated (liver, lungs, spleen, brain, heart, kidneys and testes) regardless of size. The 20 nm particles distributed mainly to liver, followed by kidneys and spleen, whereas the larger particles distributed mainly to spleen followed by liver and lung. In the other organs evaluated, no major differences between the sizes were observed. Size-dependent tissue distribution suggests size-dependent toxicity and health risks. Repeated administration resulted in accumulation in liver, lung and spleen, indicating that these organs may be potential target organs for toxicity after repeated exposure. A physiologically based pharmacokinetic (PBPK) model for nanoparticles which describes the kinetics of silver nanoparticles was developed. Model parameter values were estimated by fitting to data. No clear relation between parameter values and corresponding particle diameters became apparent.

1. Introduction

Silver nanoparticles are frequently used in consumer and medical products because of their effective antimicrobial activity [1–5]. Despite the rapidly growing share of silver-containing nanoproducts on the market [5–7], there is only limited information on the possible risks of exposure to silver nanoparticles. In a recent review evaluating the risk assessment of silver nanoparticles, different knowledge gaps were identified, including toxicokinetics [4]. Similar data gaps were identified for the possible registration of nanosilver as a substance under the EU REACH regulation [8].

The health risk is obviously related to the potential exposure of individuals to the nanomaterial. If there is no absorption, the potential risks are limited to possible local effects at the site of exposure mainly being lung, gastrointestinal tract, or skin. To date, almost all toxicological experiments dealing with nanoparticles describe the total inhaled, ingested, injected, or dermally applied dose of nanoparticles and do not investigate absorption or internal exposure. The internal exposure is that part of the external dose of nanoparticles that enters the systemic circulation and thus potentially reaches all organs and tissues.

Potential target organs for toxicity can be identified, by studying the distribution of nanoparticles over various organ systems preferably following intravenous administration. Oral, dermal and inhalation exposure to silver nanoparticles revealed distribution of these particles to several organs including liver, kidneys, lungs, heart, brain, testes, lymph nodes and skin [9–14]. Depending on the route of administration, highest concentrations were found in stomach, liver, kidneys, lungs and skin.

When using intravenous administration, absorption is bypassed and other aspects of toxicokinetic processes, such as tissue distribution and elimination, can be studied with more precision. Differences in tissue distribution between single and repeated exposure provide insight into the potential of accumulation. Furthermore, information on the time required for elimination of nanoparticles from blood and tissues provides more detailed information about the potential accumulation after repeated exposure to nanoparticles.

So far, most studies on silver nanoparticles have described the distribution of only one size of particle [9–16]. However, the size of nanoparticles can be a significant determinant of particle distribution as shown for gold nanoparticles by De Jong et al. [17] and for

* Corresponding author. Tel.: +31 30 274 23 11; fax: +31 30 274 44 46.
E-mail address: wim.de.jong@rivm.nl (W.H. De Jong).

0142-9612/$ – see front matter © 2010 Elsevier Ltd. All rights reserved.
doi:10.1016/j.biomaterials.2010.07.045

silica nanoparticles by Xie et al. [18]. In addition, information on similarities and differences in tissue distribution can aid in the discussion whether health risks differ between particles made of the same element but with different characteristics.

To obtain insight into the kinetic profile of silver nanoparticles, the aim of the present study was to determine the influence of particle size on tissue distribution and potential organ accumulation of silver nanoparticles in the rat. Rats were exposed to various sizes of silver nanoparticles (20, 80 and 110 nm) by intravenous administration once daily for 5 consecutive days. Blood kinetics and tissue distribution of silver nanoparticles were investigated up to 16 days after intravenous exposure. In order to describe the kinetics of silver nanoparticles, a physiologically based pharmacokinetic (PBPK) model was developed that fits the concentration-time course in blood, liver, spleen and kidney simultaneously. This mathematical model can be used to identify potential target organs relevant for risk assessment, and estimate levels of silver nanoparticles in several tissues after different exposure scenarios. Moreover, it can aid in the design of optimal sampling schemes and possibly in gaining insight between the kinetics of nanoparticles and their diameter.

2. Materials and methods

2.1. Animals

Six-week-old male Wistar rats (HsdCpb:WU) were purchased from Harlan Nederland BV (Horst, The Netherlands) and allowed to acclimatize for 2 weeks before starting the experiment. Animals were bred under specific pathogen-free (SPF) conditions and barrier maintained during the entire experiment in Macrolon cages at a room temperature of 23 ± 1 °C, a relative humidity of 50 ± 5% and a 12-h light/dark cycle. Drinking water and conventional feed were provided *ad libitum*. The experiment was approved by an independent Ethical Committee on Animal Experimentation and conducted in compliance with all applicable provisions of the national laws, i.e. the Experiments on Animal Decree and the Experiments on Animal Act.

2.2. Silver nanoparticles

Three different sizes (20, 80 and 110 nm) of spherical silver nanoparticles dispersed in phosphate buffer (2 mM; pH 7.4) were provided by NanoComposix, San Diego, CA, USA. The purified nanosilver dispersions were well characterized (Table 1) and no sediments or agglomerates/aggregates were visually noted.

2.3. Experimental design

Rats were divided in 4 groups: 20 nm ($n = 21$), 80 nm ($n = 21$), 110 nm ($n = 21$), and control ($n = 7$). Four days prior to the start of the experiment, a single venous blood sample (tail vein; 100 μL) was obtained from two animals in the control group. From Day 1, rats were intravenously injected (tail vein) with either 1 mL nanosilver dispersion or vehicle control (phosphate buffer) once daily for 5 consecutive days. The injections were well tolerated and no adverse effects were observed during the entire experiment. At Day 1, 3 and 5, venous blood samples were taken from the treatment-groups at $t = 2$, 5, 10, 20, 30 and 60 min after injection. Blood samples from the animals in the control group were collected at $t = 2$ min only. At 24 h (day 2), 48 h (day 3), 96 h (day 5), 120 h (day 6), 168 h (day 8), 240 h (day 11) and 384 h (day 17) *after the first injection*, rats ($n = 10$ 3 per treatment group and 1 of the control group) were anaesthetized with isoflurane (Isoflu®, AST Pharma, Oudewater, The Netherlands) in oxygen and subsequently euthanized by drawing blood from the abdominal aorta. Next to blood, liver, spleen, kidneys, lungs, heart, brain and testes were collected. Organs were weighed and homogenized. All samples were stored at −20 °C. After subjecting the sample material to a digestion process, the silver content was determined by inductively coupled plasma mass spectrometry (ICP-MS).

Table 1
Characteristics of silver nanoparticles per particle solution.

	20 nm	80 nm	110 nm
Silver particle size (nm)	20.3 ± 1.9	79.8 ± 5.1	112.6 ± 7.8
Size distribution (%)	9.2	6.4	6.9
Number of particles in injection solutions (mL^{-1})	5.0×10^{11}	9.4×10^{9}	3.5×10^{9}
Mean surface area per particle (nm^2)	1.31×10^{3}	2.01×10^{4}	4.00×10^{4}
Surface area in injection solution (nm^2/mL)	6.5×10^{14}	1.9×10^{14}	1.4×10^{14}
Silver concentration in injection solution (μg/mL)	23.8	26.4	27.6
Visual appearance injection solution	Yellow, transparent	Transparent	Transparent

2.4. Reagents, standards, and reference materials

All chemicals used for ICP-MS were of analytical grade or of high purity. Nitric acid (HNO_3) was purchased from Merck, Darmstadt, Germany. The calibration standard solution of silver (Ag), as well as a solution of the element indium (In) used as internal standard, were prepared using single element stock solutions with a concentration of 1000 μg/mL from Inorganic Ventures, supplied by Instrument Solutions, Nieuwegein, The Netherlands. Deionised water (H_2O) with 17.2 MΩcm was produced by a system from Christ, Zoeterwoude, The Netherlands. For controlling the concentration of the calibration standard solution of silver, silver nitrate ($AgNO_3$) crystalline extra pure from Merck, Darmstadt, Germany, was used. For spiking experiments the matrix of "Seronorm Trace levels in blood" (supplied by C.N. Schmidt, Amsterdam, The Netherlands) was used.

2.5. Instrumentation

A drying cabinet, Heraeus type T6060 (supplied by Thermo, Breda, The Netherlands), was used. For the digestion of the sample materials, a Stuart block heater SBH200D (supplied by Omnilabo, Breda, The Netherlands) was used. The presence of silver was measured with an inductively coupled plasma mass spectrometer ICP-MS, type ELAN DRC Plus (Perkin Elmer, Groningen, The Netherlands).

2.6. Accuracy and quality control aspects of ICP-MS

Next to the control of chemical blanks, three types of experiments were included to cover different performance characteristics and quality control aspects. However, for silver (nanoparticles) in biological materials there is no suitable reference material commercially available. The matrix effects were studied by the standard addition experiments and calculation of the recovery. Samples of liver, kidney and brain from control rats were spiked with known concentrations of the silver standard solution (absolute amount of silver: 1 μg) which was also used for the external calibration. Finally, standard addition experiments were carried out by spiking reference blood samples with the silver nanoparticles (20, 80, 110 nm) prior to sample pretreatment and analysis (data not shown).

2.7. Sample preparation prior to measurement with ICP-MS

To the homogenized organ samples (0.2–0.5 g) 0.5 mL concentrated HNO_3 was added. The samples were placed in the drying cabinet at 50 °C for 1 h to pre-dissolve the sample material. Then, the samples were transferred into digestion vials by adding three times 0.5 mL concentrated HNO_3. For other matrices the sample amount was as follows: 0.1–0.5 g blood; 0.05 g original nanoparticles (20, 80, 110 nm) or silver nitrate. To these samples 3 mL concentrated HNO_3 was added. The mixture was digested overnight with a maximum temperature of 130 °C. Afterwards the mixture was transferred into another vial, spiked with the internal standard In (final concentration: 100 μg/L) and H_2O was added to a total volume of 10 mL. The total solution was shortly shaken by hand.

2.8. Measurement with ICP-MS

The aim of this study is the identification of silver nanoparticles in different organs. As nitric acid is suitable to dissolve metallic silver, it was chosen to digest the samples. Hence, all reported concentrations are concentrations of free silver, e.g. silver nanoparticles, metallic silver and free silver ions, which are dissolvable in nitric acid. These concentrations do thus not include silver precipitations, e.g. bounded silver ions like silver chloride (AgCl), which do not dissolve in nitric acid.

Quantification was carried out by external six-point-calibration with internal standard correction. Stock solutions were diluted with approximately 20% HNO_3 to relevant concentration levels. All measurements of standards and samples were carried out with the ICP-MS system. The main instrumental operating conditions were as follows: RF power 1450 W and nebulizer gas flow 0.91 L/min Ar. The following isotopes were measured: ^{107}Ag and ^{109}Ag as well as ^{115}In as internal standard. The results of both Ag isotopes were comparable. The results of ^{109}Ag were reported and the results of ^{107}Ag were used for control.

2.9. Physiologically based pharmacokinetic (PBPK) model

A physiologically based pharmacokinetic (PBPK) model was developed. Therefore a cascade of models of increasing complexity, from 2 compartments (blood and

remaining tissues) to 5 compartments (blood, liver, spleen, kidney and remaining tissues) was developed. Model parameters fitted for a model at a lower level of complexity served as initial parameter estimates for fitting the model at the next higher level of complexity. The fully developed 5 compartment model is depicted in Fig. 1. The model contains a blood compartment for transport of the nanoparticles. As it is not possible to discriminate models with elimination from blood or from one of the tissues or from a combination of blood and tissues, for purposes of parameter identification it was chosen to model elimination from blood. This could indicate urinary clearance from blood, but it can also be interpreted as biliary clearance via the liver.

Each of the compartments, except for the remaining tissues compartment, is divided into two subcompartments, *i.e.* is described by two state variables. One state variable represents the moiety of nanoparticles that is freely available for exchange between tissue and blood, the other state variable represents the moiety that is (quasi) irreversibly incorporated into tissue. Note that, as tissues are homogenized, the experimentally determined tissue concentration is based on the sum of these two moieties. The time frame of sampling did not allow for discriminating between this modelling approach and an approach in which the latter moiety is (very) slowly released again. Not all of the remaining tissues, such as e.g. muscle, skin and bone, were sampled, so identification of the parameter value for this process of incorporation is not possible in the remaining tissues compartment. This implies that the value of the excretion rate parameter also accounts for "elimination" through incorporation in the remaining tissues, as incorporated nanoparticles do not contribute to the systemic processes any more.

A PBPK model requires physiological data of the species studied. In this case, the experimentally determined overall rat weight was assumed to be 300 g. Relative organ weights were taken from Brown et al. [19], Tables 5 and 21, to obtain weights for liver, spleen and kidneys. From the same reference, cardiac output was determined following the allometric scaling at p 441 and fractional regional blood flow for liver and kidneys was obtained from Table 23. Regional blood flow in spleen was determined by the value of 0.71 mL/g tissue per minute in Vaupel et al. [20] and spleen weight as determined above. Each rat was assumed to be administered the amount of silver nanoparticles as reported in Table 1. All other parameter values had to be estimated from the experimental data. Rat physiological parameters used for development of the compartment model are presented in Table 2. Weight of blood, liver, spleen and kidneys together, represent only 12% of total body weight. Blood flow through liver, spleen and kidneys represent 33% of total blood flow.

The model was implemented in ACSL-model and parameter fitting was done with the ACSL-optimize module in ACSL-math.

The estimation procedure started with the simplest 2 compartment model with blood and all other remaining tissues as the physiological compartments. This involves the three parameters for partition, flow limitation and systemic elimination, P_r, f_{Qr}, k_b respectively to be fitted. Then, the remaining tissues compartment was split up into a liver and other remaining tissues compartment, so three compartments in total. This involves fitting three additional parameters for partition, flow limitation and (quasi-) irreversible tissue incorporation, P_l, f_{Ql}, $k_{l,x}$ respectively, but with the first three parameters, P_r, f_{Qr}, k_b possessing a rather accurate initial estimate. Then, the remaining tissues compartment was split up into spleen and other remaining tissues. The values found for the liver compartment, P_l, f_{Ql}, $k_{l,x}$ were held fixed and those for spleen, P_s, f_{Qs}, $k_{s,x}$ were fitted together with the values P_r, f_{Qr}, k_b, again possessing rather accurate initial estimates. These steps were repeated up to a maximum of 5 compartments. Note that because in each state the remaining tissue compartment differs from its predecessor, its parameter values have to be fitted anew together with those for the newly introduced compartment.

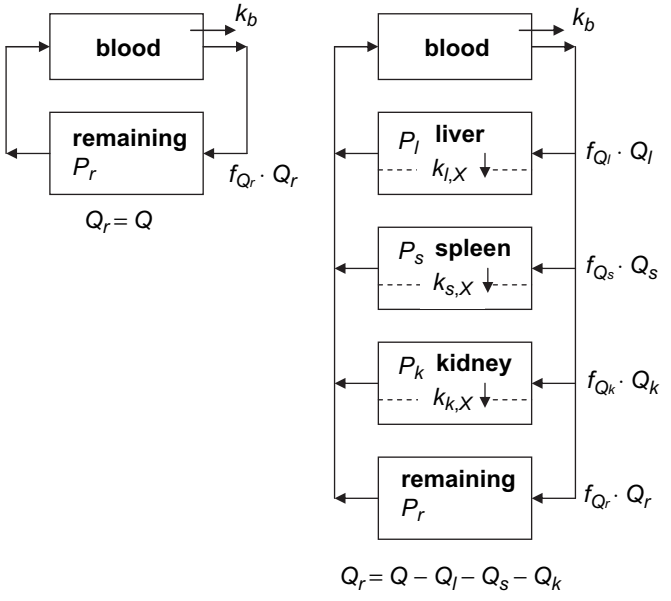

Fig. 1. Compartment model for the kinetics of silver nanoparticles. Left: simple 2 compartment model for initial parameter estimation; right: most complex 5-compartment model. The *P*'s denote distribution coefficients, the *Q*'s (regional) blood flows, the *f*'s flow limiters and the *k*'s elimination (from blood) and (quasi-)irreversible tissue incorporation.

Table 2
Rat physiological parameters.

	Total	Blood	Liver	Spleen	Kidneys	Remaining
Weight (g)	300	22.2	10.2	0.6	2.1	264.9
Flow (mL/h)	5700	–	1043	26	804	3827

3. Results

3.1. Blood concentration-time curve

In all blood samples, silver concentration was measured and expressed per gram blood. The blood concentration-time curves revealed a rapid decline in silver concentration during the first 10 min after injection (Fig. 2). After 10 min, blood concentrations of all sizes analysed remained rather stable, although slightly higher concentrations were found following repeated injection, independent of size.

3.2. Tissue distribution

Silver concentrations were measured in blood, liver, lungs, spleen, brain, heart, kidneys and testes. After both single and repeated injection, silver could be detected in all organs evaluated, regardless of particle size administered. In control rats, silver was not detected in any organ (data not shown).

Silver concentrations per gram organ are displayed in Fig. 3 (single exposure in A, repeated exposure in B) and Fig. 4 (over time).

Fig. 3A shows the mean silver concentrations per gram organ after one single injection (day 2). Following single exposure, highest silver concentrations per gram organ were found in spleen followed by liver for both 80 and 110 nm particles. For 20 nm particles, highest concentration per gram organ was found in liver only, although at a lower level compared to the larger particles. Concentrations in liver increased with particle size (169, 539 and 1077 ng/g liver for 20, 80 and 110 nm particles, respectively). Concentrations in spleen were remarkably lower (~20 fold) for 20 nm particles compared to the larger particles. In the other organs evaluated (kidney, heart, lungs, testes and brain) silver concentrations were much lower and comparable for all sizes. In brain (all sizes) and heart (20 nm only), silver concentrations were close to the limit of quantification.

Fig. 3B shows the mean silver concentrations per gram organ after 5 consecutive injections (day 6). At this time point, silver concentrations were comparable for 80 and 110 nm particles in all organs, while concentrations for 20 nm particles generally showed a different picture. Similar to the results after single injection, highest silver concentrations were found in spleen followed by liver after repeated injection of 80 and 110 nm particles and in liver only after repeated injection of 20 nm particles.

At autopsy as much blood as possible was collected to maximize removal of residual blood from the organs. In the measured tissue concentrations, the amount of residual blood present in these tissues is included. Hence, the latter could have been overestimated.

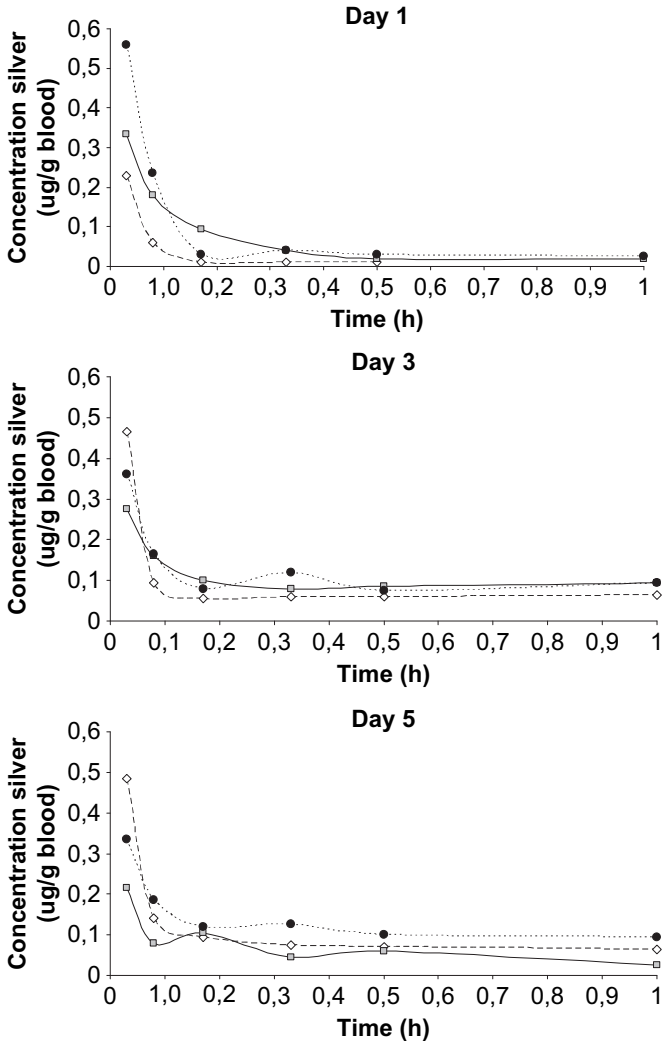

Fig. 2. Blood concentration-time curves at day 1, 3 and 5. 20 nm: open diamond, 80 nm: grey square, 110 nm: closed circle ($n = 2$ for each time point).

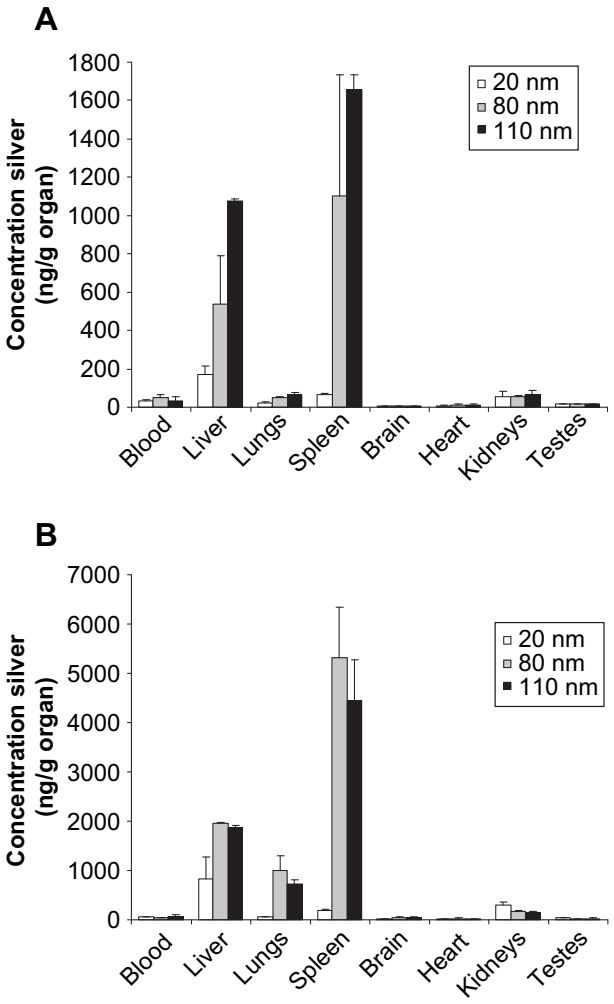

Fig. 3. Mean silver concentrations (ng) per gram organ after one single injection (A) and 5 consecutive injections (B). 20 nm: white bars, 80 nm: grey bars, 110 nm: black bars; $n = 3$, error bars represent standard deviations.

However, some organs with high-blood content (liver, spleen) show much higher silver concentrations than blood, suggesting that residual blood in these organs had only a negligible effect on the amount of silver measured. On the other hand, the concentrations found in testes, heart and brain were low, even compared to the concentrations found in blood. Therefore, contribution of residual blood cannot be ruled out for these organs.

Fig. 4 shows the mean silver concentration per gram organ over time for all particles and all organs evaluated. Following repeated exposure (5 consecutive days), silver concentrations were higher in all organs compared to single exposure. For 20 and 80 nm particles, silver concentrations increased from day 2, with a peak concentration for all organs at day 6. For 110 nm particles, peak concentrations were observed in testes at day 3, in liver, brain and heart at day 5, in spleen and lungs at day 6 and in kidneys at day 11. Highest blood concentrations were reached at day 6, 3 and 5 for the 20, 80 and 110 nm particles, respectively and gradually decreased to below the limit of quantification at the end of the experiment. In spleen and lungs, silver concentrations of 80 and 110 nm particles remained comparable until day 8, whereas from day 8 until the end of the experiment, higher concentrations were found for 80 nm compared to 110 nm particles. In liver, higher concentrations were measured for 110 nm particles until day 5, whereas from day 6 until the end of the experiment, silver concentrations were comparable between both particle sizes. After the final repeated injection of 80 and 110 nm particles, silver concentrations in liver, lungs and spleen gradually decreased towards the end of the experiment, although still high levels were measured at day 17. During the whole experiment, concentrations for the 20 nm particles were remarkably lower in these organs. With respect to kidneys, heart, brain and testes, no major differences were observed between the particles sizes tested.

Table 3 describes the silver concentration per organ over time. For all particle sizes, highest concentrations were found in liver at all days. Next to liver, high silver concentrations were also found in blood and kidneys for 20 nm particles, in blood, lungs, spleen and heart for 80 nm particles and in spleen, blood, kidneys and lungs for 110 nm particles.

Overall, silver concentrations for 20 nm particles were remarkably lower in all organs, except blood, compared to the larger particles. In addition, for 80 nm particles higher concentrations were found in lungs and heart compared to 110 nm particles, whereas for the 110 nm particles higher concentrations were measured in spleen and kidneys compared to the 80 nm particles. Nevertheless, liver contributed by far the most to the total of the silver concentrations for all particle sizes.

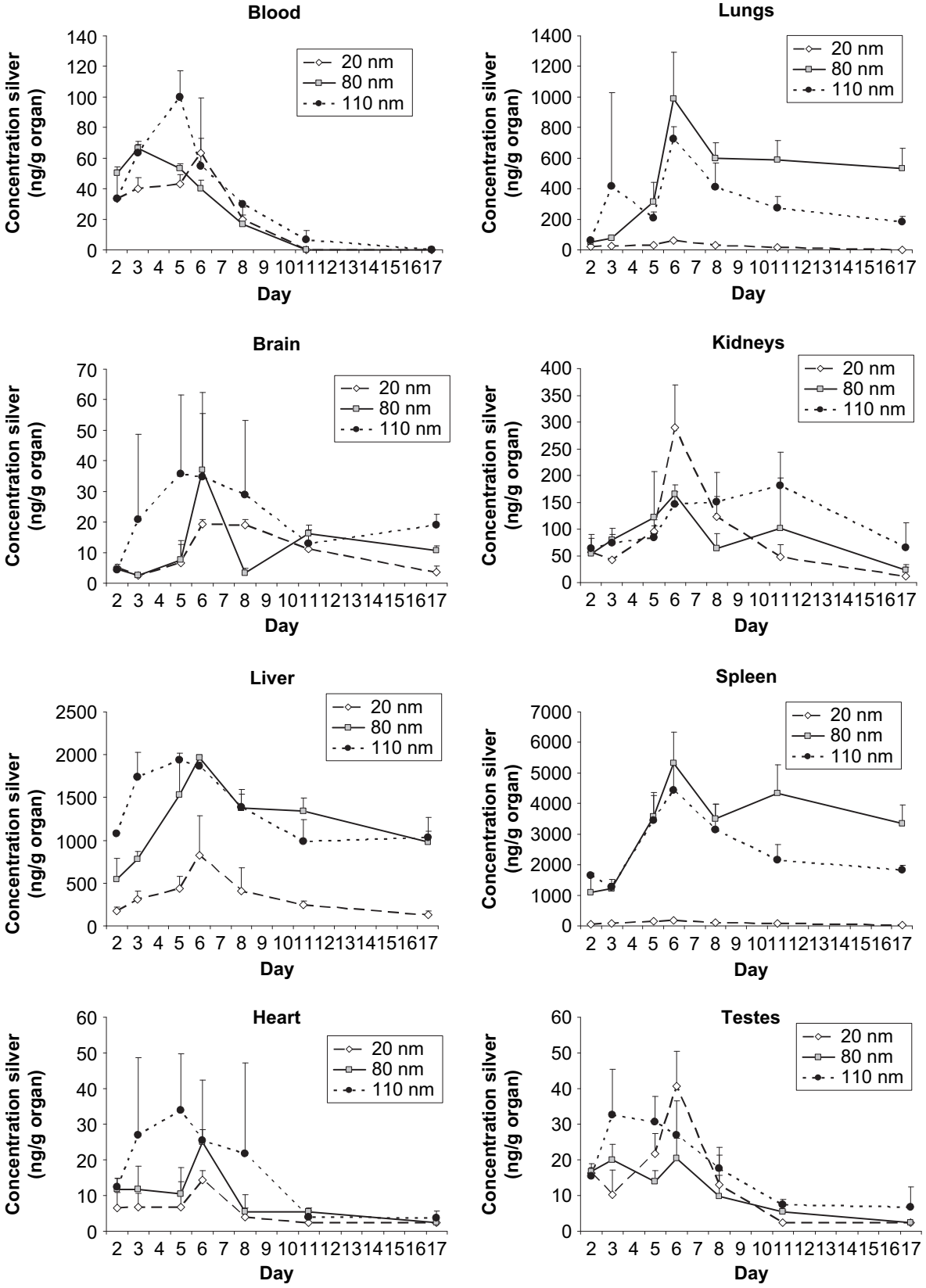

Fig. 4. Mean silver concentrations (ng) per gram organ over time. 20 nm: open diamond, 80 nm: grey square, 110 nm: closed circle; $n = 3$, error bars represent standard deviations.

Table 3A
Mean silver concentrations (ng per organ, mean ± standard deviation), the total level of silver determined in all organs (ng), and the recovered percentage of the cumulative dose for 20 nm particles (23.8 μg/injection, $n = 3$).

20 nm	Day 2	Day 3	Day 5	Day 6	Day 8	Day 11	Day 17
Blood	602 ± 98	720 ± 23	784 ± 210	1143 ± 117	359 ± 9	0 ± 0	0 ± 0
Liver	2326 ± 676	3872 ± 1101	5564 ± 1966	10968 ± 5693	5006 ± 2684	3192 ± 505	1855 ± 745
Lungs	31 ± 11	34 ± 4	41 ± 20	77 ± 6	39 ± 2	23 ± 6	3 ± 0
Spleen	38 ± 5	47 ± 2	84 ± 20	106 ± 23	62 ± 3	42 ± 27	17 ± 3
Brain	8 ± 1	5 ± 0	12 ± 13	35 ± 5	35 ± 2	20 ± 14	7 ± 4
Heart	7 ± 5	7 ± 4	6 ± 6	13 ± 3	4 ± 2	2 ± 0	3 ± 0
Kidneys	110 ± 45	85 ± 8	198 ± 48	605 ± 187	264 ± 167	99 ± 53	28 ± 37
Testes	48 ± 7	33 ± 22	66 ± 22	126 ± 30	45 ± 8	8 ± 1	8 ± 1
Total of Ag in organs (ng)	3170	4803	6755	13074	5814	3387	1920
% of cumulative dose	13 ± 3	10 ± 2	7 ± 2	11 ± 5	5 ± 2	3 ± 0	2 ± 1

3.3. Total silver levels in organs

Calculating the amount of silver detected in the investigated organs as percentage of the injected dose, the highest percentage is recovered from the liver, regardless of particle size (Table 3). Less then 1% of the injected dose ends up in the lungs, brain, heart, kidneys and testes for 80 and 110 nm particles, only a few percent of the injected dose is retrieved from the spleen. The total percentage of silver recovered from the organs is higher after single exposure compared to 5 consecutive injections, which is inherent to the way of calculating. The dose administered to one animal is about 25 μg (Table 1). After 24 h for example 33% of the injected dose (80 nm, day 2; Table 3) is recovered from the investigated organs. Subsequently a second dose is administered, thus in total a dose of 50 μg is administered, but part of this dose is already released during the first 24 h. Hence, when the total amount of the silver recovered from the organs is calculated as a percentage, the percentage decreases, whereas the absolute amount of silver recovered from the organs increases.

After single exposure, total recovery was lowest for 20 nm particles (13%), followed by 80 nm particles (33%) and 110 nm particles (55%). After repeated dosing, total recovery was still lowest for 20 nm particles (11%), but comparable for 80 and 110 nm particles (22% and 21%, respectively).

3.4. Elimination

Following the last injection, silver concentration decreased in all organs regardless of particle size, except for 110 nm particles in kidneys (highest concentration measured at day 10) (Fig. 4 and Table 3). However, at the end of the experiment (day 17, e.g. 12 days after the last administration), high silver concentrations were still measured in liver, lungs and spleen for both 80 and 110 nm particles. At this time point, silver concentrations were also measured in kidneys and brain, although at much lower levels. Regarding the 110 nm particles, even all organs contained silver at day 17. These results indicate that silver nanoparticles, and especially the 110 nm particles, are slowly eliminated from the organs.

3.5. Accumulation

Increased silver concentrations in tissues after repeated exposure indicate accumulation. Accumulation is presented in Fig. 4, by comparing concentrations at day 2 (after single dose) to day 6 (following repeated doses). Accumulation occurs in all organs regardless of particle size, except for 80 nm in blood. Most accumulation was observed in the lungs for 80 nm (factor 20) and 110 nm (factor 11.5). For 20 nm particles, most accumulation was found in kidneys (factor 5.5) and liver (factor 5). No clear trends with either particle size or organ were observed, although silver accumulates in the brain with a rather high factor for 20 nm (factor 4), 80 nm (factor 7) and 110 nm (factor 8).

3.6. Physiologically based pharmacokinetic (PBPK) model

A modelling approach of PBPK-like compartment models of increasing complexity from 2 to 5 compartments proved to be successful for the identification of determinants of the biokinetics of nanoparticles. Four processes can be distinguished that determine blood and tissue concentrations after intravenous exposure:

- transport of particles from blood to tissues
- partitioning between tissues and blood
- elimination from blood
- (quasi)-irreversible incorporation in tissues

The model combines the description of disposition of nanoparticles and dissolved (parts) of particles in terms of processes known from the disposition of conventional substances with a minimal number of parameters needed. Fitted parameters values are depicted in Table 4. The comparison of model and experimental

Table 3B
Mean silver concentrations (ng per organ, mean ± standard deviation), the total level of silver determined in all organs (ng), and the recovered percentage of the cumulative dose for 80 nm particles (26.4 μg/injection, $n = 3$).

80 nm	Day 2	Day 3	Day 5	Day 6	Day 8	Day 11	Day 17
Blood	896 ± 303	1188 ± 118	980 ± 92	684 ± 5	296 ± 92	0 ± 0	0 ± 0
Liver	6968 ± 3231	9695 ± 1346	19756 ± 4979	23880 ± 964	16947 ± 1063	16262 ± 2222	13315 ± 1649
Lungs	603 ± 356	692 ± 148	2153 ± 397	3021 ± 591	1915 ± 500	2554 ± 715	1982 ± 190
Spleen	110 ± 22	160 ± 46	256 ± 178	327 ± 39	135 ± 64	217 ± 211	47 ± 18
Brain	10 ± 3	10 ± 6	9 ± 6	22 ± 16[a]	5 ± 5	5 ± 0	2 ± 0
Heart	63 ± 11	132 ± 41	457 ± 180	1272 ± 455	749 ± 134	754 ± 131	676 ± 140
Kidneys	9 ± 1	5 ± 0	13 ± 9	66 ± 43	6 ± 2	31 ± 2	20 ± 3
Testes	53 ± 6	62 ± 16	44 ± 7	65 ± 21	32 ± 38	17 ± 1	8 ± 1
Total of Ag in organs (ng)	8712	11944	23668	29337	20085	19840	16051
% of cumulative dose	33 ± 10	23 ± 2	22 ± 5	22 ± 1	15 ± 1	15 ± 2	12 ± 1

[a] $n = 2$.

Table 3C
Mean silver concentrations (ng per organ, mean ± standard deviation), the total level of silver determined in all organs (ng), and the recovered percentage of the cumulative dose for 110 nm particles (27.6 μg/injection, $n = 3$).

110 nm	Day 2	Day 3	Day 5	Day 6	Day 8	Day 11	Day 17
Blood	582 ± 358	1115 ± 145	1781 ± 287	1016 ± 819	565 ± 18	117 ± 101	0 ± 0
Liver	13381 ± 567	22115 ± 3108	23040 ± 65	24480 ± 1536	18191 ± 3489	11748 ± 3382	13731 ± 3896
Lungs	129 ± 60	154 ± 49	170 ± 36	309 ± 48	314 ± 5	386 ± 100	140 ± 105
Spleen	859 ± 34	690 ± 83	1985 ± 541	2558 ± 543	1771 ± 481	1403 ± 267	1150 ± 32
Brain	8 ± 1	39 ± 52	68 ± 50	65 ± 39	53 ± 44	22 ± 7	36 ± 6
Heart	11 ± 3	23 ± 20	30 ± 15	24 ± 2	21 ± 24	4 ± 3	4 ± 2
Kidneys	83 ± 27	730 ± 1094	316 ± 51	960 ± 122	528 ± 165	347 ± 130	221 ± 23
Testes	44 ± 9	63 ± 61	100 ± 26	85 ± 29	51 ± 25	24 ± 3	23 ± 18
Total of Ag in organs (ng)	15098	24929	27491	29497	21494	14052	15303
% of cumulative dose	55 ± 0	45 ± 7	25 ± 1	21 ± 2	16 ± 3	10 ± 2	11 ± 3

data are shown in Figs. 5–7 for the 20, 80 and 110 nm diameter particles, respectively. In these figures, the panels in the top row and at the middle row left show the result in blood on logarithmic time scale relative to the hours 0, 48 and 96, i.e. time points at which silver nanoparticles are administered. Presentation on linear time scale is not informative, as the time resolution on linear scale is inadequate for the comparison of model calculations and experimental data due to the abundance of data during the first hours after administration. The other panels are presented on linear scale. Sampled concentrations at the time points 24, 48 and 96 h should be compared to the local minima at those times of the model calculations.

The data and the model results are in good agreement with each other. Especially when considering the fact that the model simultaneously estimates concentrations in blood and tissues.

The described accumulation in tissues is confirmed by the kinetic modelling of the data. For the 20 nm particles, about 20% of the highest concentration (~1800 ng = 1.3% of total dose of 118 μg administered during 5 consecutive days) is quasi-irreversibly retained in liver, whereas negligible amounts are retained in spleen and kidney. For the 80 nm particles, about 40% of the highest concentration in liver (8.3% of total dose), 70% of the highest concentration in spleen (1.5% of total dose) and 20% of the highest concentration in kidney (0.1% of total dose) is quasi-irreversibly retained. For the 110 nm particles, about 30% of the highest concentration in liver (5.6% of total dose), 40% of the highest concentration in spleen (0.7% of total dose) and 40% of the highest concentration in kidney (0.2% of total dose) is quasi-irreversibly retained. Thus, the total amounts that are quasi-irreversibly retained in the sampled tissues are 1.3% for the 20 nm, 9.9% for the 80 nm and 6.5% for the 110 nm particles.

Table 4
Fitted parameter values (±s.e.).

Parameter	20 nm	80 nm	110 nm
k_b (h^{-1})	0.55 ± 0.03	0.57 ± 0.02	0.45 ± 0.02
P_l	10 ± 2	17 ± 2	22.6 ± 0.1
f_{Ql}	0.12 ± 0.04	0.244 ± 0.002	0.253 ± 0.002
$k_{l,x}$ (h^{-1})	0.002 ± 0.001	0.008 ± 0.001	0.0029 ± 0.0004
P_s	2.9 ± 0.3	28 ± 7	42 ± 3
f_{Qs}	0.07 ± 0.29	1 (fixed value)	0.036 ± 0.005
$k_{s,x}$ (h^{-1})	0.0013 ± 0.0005	0.015 ± 0.004	0.0036 ± 0.001
P_k	3.3 ± 0.6	2.07 ± 0.03	0.90 ± 0.04
f_{Qk}	0.009 ± 0.019	0.83 ± 0.1	0.24 ± 0.01
$k_{k,x}$ (h^{-1})	0.0008 ± 0.0010	0.003 ± 0.001	0.011 ± 0.001
P_r	2.8 ± 0.3	1.1 ± 0.2	1.2 ± 0.1
f_{Qr}	0.20 ± 0.01	0.112 ± 0.001	0.11 ± 0.01

k_b is the apparent clearance from blood. For the compartments liver, spleen, kidney and remaining tissues (subscripts l, s, k and r, respectively) the tissue blood partition P, the flow rate limiter f and the the rate of quasi-irreversible tissue incorporation k is presented. The latter cannot be identified for the remaining tissues compartment.

4. Discussion

This study describes the tissue distribution and accumulation of intravenously administered silver nanoparticles of various sizes (10, 80 and 110 nm) in the rat.

After each injection, a rapid decline in blood silver concentrations was noted within 10 min following injection, suggesting that silver nanoparticles rapidly distribute to tissues. Following both single and repeated treatment, silver nanoparticles distributed to all organs evaluated (liver, spleen, kidneys, lung, heart, brain and testes) regardless of size. This is in agreement with previous reports describing distribution of silver nanoparticles to multiple organs including liver, kidneys, heart, lungs, brain, testes, lymph nodes and skin [9–14]. Depending on the route of administration, highest concentrations were found in stomach, liver, kidneys, lungs and skin.

Distribution of 20 nm silver particles appears to be different from the larger particles. The 20 nm particles distributed mainly to liver, followed by kidneys and spleen, whereas the larger particles distributed mainly to spleen followed by liver and lung. In the other organs investigated, no major differences between the sizes were observed. This difference in tissue distribution between 20 nm particles and the larger particles were observed throughout the whole duration of the experiment. Size-dependent tissue distribution suggests size-dependent toxicity and health risks. A different distribution pattern for 20 nm versus 80 and 110 nm also indicates that it is unlikely that the silver nanoparticles all immediately dissolved into silver ions, as this would have resulted in a similar distribution pattern regardless of the size of the nanoparticles. This suggests that grouping of nanoparticles solely by chemical composition is not possible. Therefore, additional information should be gathered when and why nanoparticles show differences in kinetics and toxicity.

For all time points investigated silver concentrations of 20 nm particles in liver, spleen and lung were remarkably lower compared to the larger particles resulting in a rather low recovery for the 20 nm particles. Possible explanations for this finding may be faster elimination/excretion of the 20 nm nanoparticles, dissolution of (a fraction of the) silver particles to silver ions, or distribution of 20 nm particles to other organs not evaluated in this study such as skin, muscles, bone and lymph nodes. Distribution of silver nanoparticles to these other organs was previously observed in rats [9,13,14].

The cut-off size for renal excretion of quantum dots is approximately 5.5 nm [21]. If renal excretion is related to particle size only, e.g. the conclusion of Choi et al. for quantum dots also holds for silver nanoparticles, this suggests that the tested particles in this study are not excreted by urine, but via faeces or even another route. However, it is possible that the particles are partly dissolved into silver ions, which could be excreted by urine.

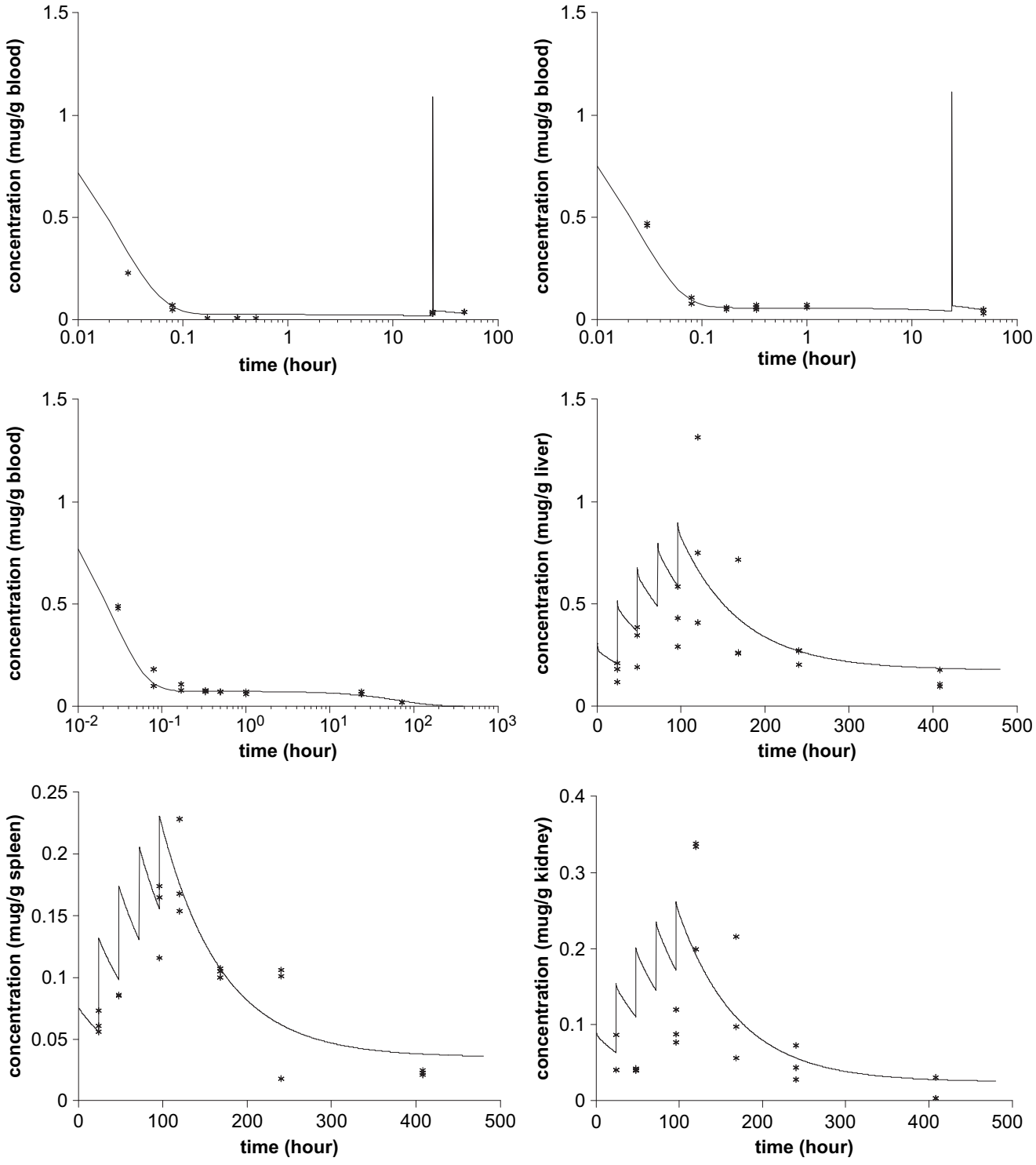

Fig. 5. Comparison of experimental data (symbols) and fitted model (straight line) presented as μg/g organ in blood, liver, spleen and kidney for the 20 nm particles. For blood, the time scale is logarithmic as to better resolve data shortly after administration. At the right upper panel administration time is 48 h and at the left middle panel 96 h. Note carefully that for liver, spleen and kidney, the experimental data at 24, 48 and 96 h should be compared with the model value at its local minimum as sampling occurred 24 h after the last injection.

For the first time, a physiologically based pharmacokinetic (PBPK) model was developed for silver nanoparticles. The PBPK model was based on the observed tissue distribution data for silver as determined by ICP-MS and uses a minimal number of parameters in terms of processes known from the disposition of conventional substances. In most of the PBPK models in literature for conventional substances, it is tacitly assumed that the rate limiting process in exchange between tissue and blood is the perfusion of the tissues. However, for nanoparticles, it might be possible that the blood-tissue barrier or transport in the tissue from this barrier to other sites is limiting due to the fact that we are dealing with nanoparticles, relatively large compared to dissolved molecules,

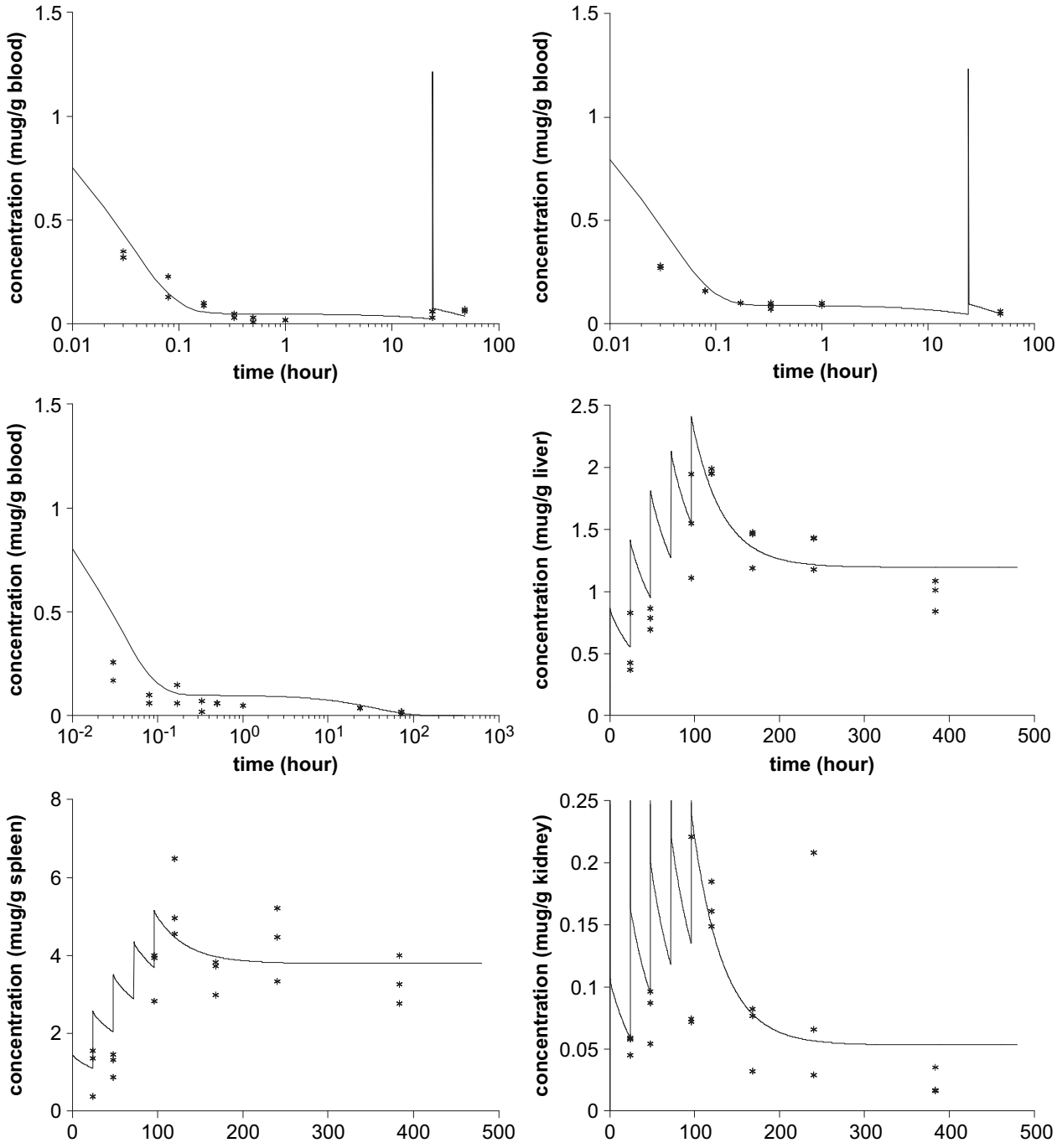

Fig. 6. Comparison of experimental data (symbols) and fitted model (straight line) presented as μg/g organ in blood, liver, spleen and kidney for the 80 nm particles. For blood, the time scale is logarithmic as to better resolve data shortly after administration. At the right upper panel administration time is 48 h and at the left middle panel 96 h. Note carefully that for liver, spleen and kidney, the experimental data at 24, 48 and 96 h should be compared with the model value at its local minimum as sampling occurred 24 h after the last injection.

and possibly still larger aggregates or agglomerates of these nanoparticles. So, we considered it necessary to introduce a transport parameter additional to the physiologically known parameter for blood flow.

The concept of partitioning between tissues and blood is clear for conventional substances and is based on the chemical potential of molecules in different phases such as water, fat and protein phase. It is less clear what determines the partition of nanoparticles but we can assume that hydrophilicity and lipophilicity are important factors. Anyway, an equilibrium of concentrations of exchangeable moieties of nanoparticles in tissue and blood can be described by a steady concentration ratio referred to as partition.

PBPK modelling of the experimental data did not reveal an unambiguous route of elimination. Hence, blood was chosen as the eliminating organ as other types of elimination would also deplete nanoparticles from blood. Moreover, this leaves open the possibility of renal and biliary clearance. It should be noted that from the point of view of the blood compartment also the (quasi-)irreversible

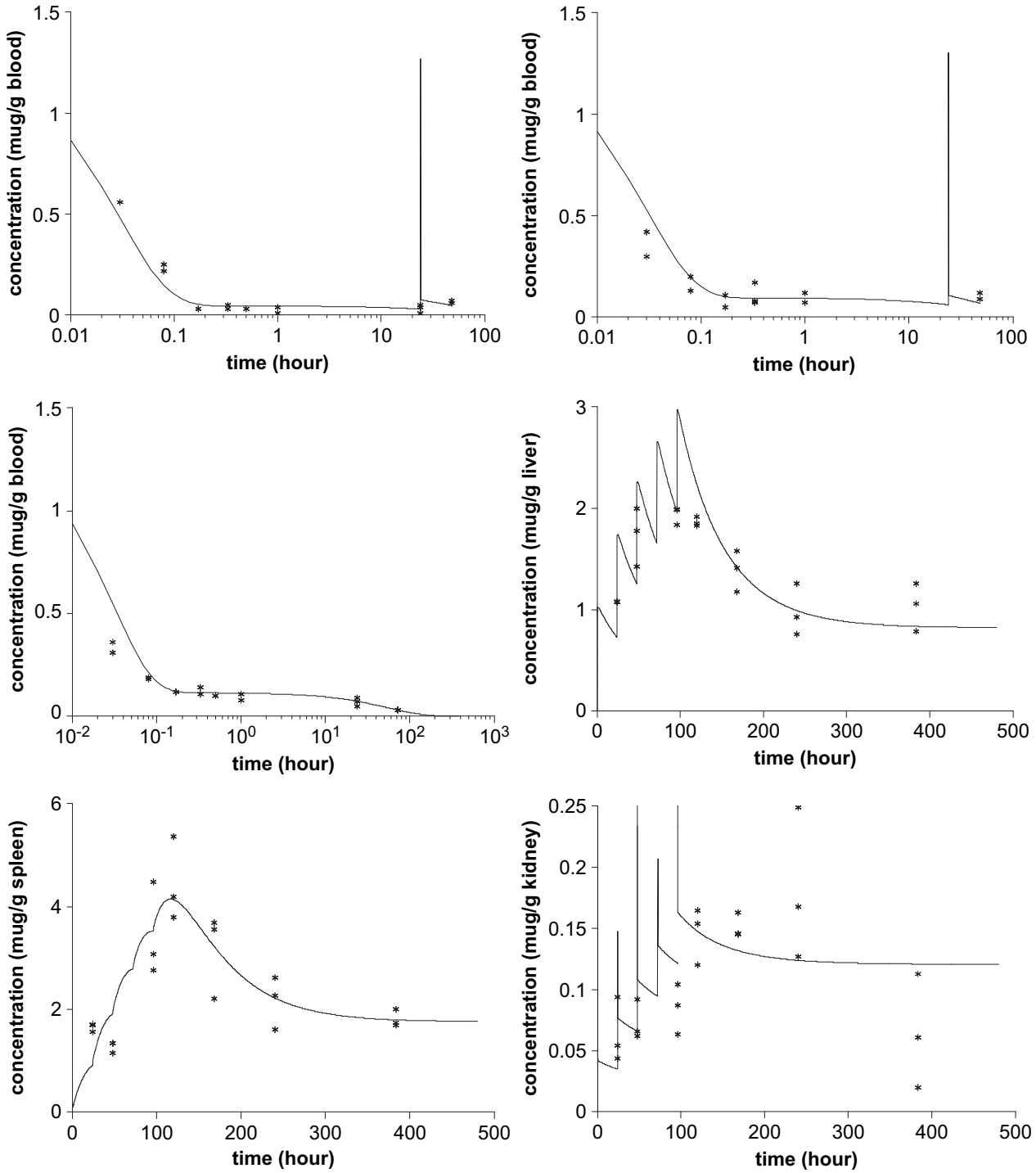

Fig. 7. Comparison of experimental data (symbols) and fitted model (straight line) presented as μg/g organ in blood, liver, spleen and kidney for the 110 nm particles. For blood, the time scale is logarithmic as to better resolve data shortly after administration. At the right upper panel administration time is 48 h and at the left middle panel 96 h. Note carefully that for liver, spleen and kidney, the experimental data at 24, 48 and 96 h should be compared with the model value at its local minimum as sampling occurred 24 h after the last injection.

incorporation in tissues is simply elimination. Generally, the model outcome in blood compares very well to the experimental data. Comparison of the model with data in the tissues is less favourable, but still quite acceptable. There is no systematic error detectable between the results for the three different diameter nanoparticles.

The model did not indicate clear relationships between nanoparticle size and its corresponding kinetic characteristics. This may be due to the fact that not only particle size but also other characteristics such as surface charge, surface coating, protein absorption or the tendency of aggregation/agglomeration in plasma, interstitial or cell fluids may be involved.

In the present study, a major fraction of the silver nanoparticles distributed to liver and spleen. Most types of nanomaterials mainly end up in liver and spleen as major organs of the reticulo-endothelial system (RES) that is dedicated to removal of agents form the blood. For example, uptake of nanoparticles by mainly liver and

spleen is also found for other nanoparticles such as silica, titanium dioxide, quantum dots, gold and iron oxide [17,18,22–25]. In addition, size-related distribution over these organs is also described by Wang et al. [22], De Jong et al. [17], Li and Huang [27], Mikhail and Allen [25] and Xie et al. [18]. Li and Huang [27] suggested that tissues with a fenestrated or incomplete endothelial lining, such as liver and spleen, respectively, contribute to a significant uptake of nanoparticles. Moreover, they conclude that particles smaller than the pore size of liver fenestrae (~ 100 nm) lead to enhanced liver uptake, whereas larger particles lead to enhanced spleen uptake, which is in agreement with our findings that show that the 20 nm particles mainly distributed to liver, whereas the larger particles mainly distributed to spleen.

Similar to other nanoparticles, such as quantum dots [23], silica [18] and gold [26], we found that the silver nanoparticles slowly eliminated from the RES containing tissues.

In the present study, repeated administration resulted in significant accumulation in liver, lung, and spleen. For the other organs a less clear accumulation pattern was observed. Accumulation indicates that silver was not completely eliminated from the tissues after the previous injection given 24 h before. Accumulation of silver nanoparticles was already described by Kim et al. [14] after repeated oral administration of silver nanoparticles (60 nm) to rats. They showed dose-dependent accumulation in blood, lungs, kidneys, brain, olfactory bulb and liver. In man, accumulation of silver nanoparticles was also reported following orally ingested colloidal silver resulting in a blue-grey hyperpigmentation of the skin [10,11]. These reports suggest that ingested colloidal silver is absorbed by the gastrointestinal tract, systemically distributed and accumulated in several tissues.

The observed accumulation of silver after repeated exposure indicates that extra attention should be paid to investigate the potential toxicity after chronic exposure to silver nanoparticles. Although the toxicity of nanosilver has been studied [reviewed in 4], effects of size on potential distribution and toxicity have not been considered. Also a comparison of nanosilver toxicity in vivo to conventional soluble silver has not yet been conducted. Therefore, further research on kinetics, toxicity and risks in relation to the size of silver nanoparticles and conventional silver with special focus on chronic exposure is recommended. In such studies it is recommended to include small silver nanoparticles (like 20 nm) in view of their specific tissue distribution, and thus potential toxicity, compared to larger nanoparticles. The possible role of dissolution of silver ions needs specific attention when considering the low overall silver recovery for the 20 nm silver nanoparticles.

Previously we reported on the tissue distribution of gold nanoparticles, in which only the smallest particles (10 nm) showed the most widespread organ distribution, whereas the larger particles (>50 nm) solely distributed to liver, spleen and blood [17]. In the present study, all three nanosilver sizes showed a more widespread organ distribution than solely to liver and spleen. This difference in tissue distribution might be related to the composition and other characteristics of gold versus silver nanoparticles. Gold particles are generally believed to be more inert than silver nanoparticles. The reactive silver particles might interact with proteins and lipids present in the biological fluid. These interactions lead to the formation of protein or lipid coronas that can adversely affect biological processes like tissue distribution [28,29]. Another explanation might be by the solution used for dispersion of the nanoparticles. Gold nanoparticles were injected following dispersion in phosphate buffered saline (PBS), whereas silver nanoparticles were dispersed in a phosphate buffer without saline. A preliminary study with silver nanoparticles (20, 80 and 110 nm) dispersed in PBS showed aggregation and/or agglomeration of the larger silver nanoparticles immediately after dispersion. The 80 and 110 nm particles formed aggregates of about 400–600 nm, whereas the 20 nm particles remained the same size. In this study, the 20 nm silver nanoparticles dispersed in PBS distributed to multiple organs, whereas the larger particles remained in liver, spleen and blood. Although also for the gold nanoparticles some agglomeration was observed, this mainly occurred for the smallest gold particles (10 nm) which still showed the most widespread tissue distribution [17]. This indicates the difference in tissue distribution between silver and gold nanoparticles is probably based on differences in characteristics between silver and gold particles. The well characterized saline-free phosphate buffer dispersion with silver nanoparticles used in the present study did not show any agglomeration or aggregation. Hence, the size-dependent differences in tissue distribution found in the present study cannot be related to agglomeration or aggregation of the particles in the dispersion.

5. Conclusions

After injection, all three sizes (20, 80, and 110 nm) of silver nanoparticles are rapidly removed from the blood and widely distributed to all organs evaluated. Based on levels per gram organ the distribution of the 20 nm particles appears to be different from the larger particles, suggesting that they may also show a different toxicity and thus might be associated with a different health risk. Accumulation is observed after repeated intravenous injection of silver nanoparticles generally with a peak level after the last dosing at day 5, subsequently followed by a gradual decrease. Accumulation was present in all organs, but most significantly in liver, lungs and spleen and thus these organs may be potential target organs for toxicity after repeated exposure. The developed PBPK mathematical model may be useful in designing toxicity studies as the information on the kinetics in blood and tissues can provide crucial information and understanding by estimating exposure levels in potential target organs for specific exposure scenarios.

Acknowledgements

The authors would like to acknowledge Mr. H. Strootman, Mr. R. Vlug, Mr. H. Verharen, Mr. B. Verlaan, Mrs. L. de la Fonteijne and Mr. N. van Oijen for their technical assistance during the animal experiments and prof. Dr. H. van Loveren and Dr. A. Sips for critically reviewing the manuscript.

References

[1] Roszek B, De Jong WH, Geertsma RE. Nanotechnology in medical applications: state-of-the-art in materials and devices. RIVM report 265001001. Available at: http://www.rivm.nl/bibliotheek/rapporten/265001001.html; 2005.
[2] Chen X, Schleusener HJ. Nanosilver: a nanoproduct in medical application. Toxicol Lett 2008;176(1):1–12.
[3] Rai M, Yadav A, Gade A. Silver nanoparticles as a new generation of antimicrobials. Biotechnol Adv 2009;27(1):76–83.
[4] Wijnhoven SWP, Peijnenburg WJGM, Herberts CA, Hagens WI, Oomen AG, Heugens EHW, et al. Nano-silver – a review of available data and knowledge gaps in human and environmental risk assessment. Nanotox 2009;3(2):1–30.
[5] Wijnhoven SWP, Dekkers S, Hagens WI, De Jong WH. Exposure to nanomaterials in consumer products. RIVM report 340370001. Available at: http://www.rivm.nl/bibliotheek/rapporten/340370001.html; 2009.
[6] Dekkers S, Prud'homme De Lodder LCH, De Winter R, Sips AJAM, De Jong WH. Inventory of consumer products containing nanomaterials. RIVM report 340120001. Available at: http://www.rivm.nl/bibliotheek/rapporten/340120001.html; 2007.
[7] Woodrow Wilson International Centre for Scholars. Project on emerging nanotechnologies. Consumer products inventory of nanotechnology products. Available at: http://www.nanotechproject.org/inventories/consumer/; 2009.
[8] Pronk MEJ, Wijnhoven SWP, Bleeker EAJ, Heugens EHW, Peijnenburg WJGM, Luttik R, et al. Nanomaterials under REACH. Nanosilver as a case study. RIVM report 601780003. Available at: http://www.rivm.nl/bibliotheek/rapporten/601780003.html; 2009.

[9] Takenaka S, Karg E, Roth C, Schulz H, Ziesenis A, Heinzmann U, et al. Pulmonary and systemic distribution of inhaled ultrafine silver particles in rats. Environ Health Perspect 2001;109(Suppl. 4):547–51.
[10] White JM, Powell AM, Brady K, Russell-Jones R. Severe generalized argyria secondary to ingestion of colloidal silver protein. Clin Exp Dermatol 2003;28(3):254–6.
[11] Chang AL, Khosravi V, Egbert B. A case of argyria after colloidal silver ingestion. J Cutan Pathol 2006;33(12):809–11.
[12] Trop M, Novak M, Rodl S, Hellbom B, Kroell W, Goessler W. Silver-coated dressing acticoat caused raised liver enzymes and argyria-like symptoms in burn patient. J Trauma 2006;60(3):648–52.
[13] Ji JH, Jung JH, Kim SS, Yoon JU, Park JD, Choi BS, et al. Twenty-eight-day inhalation toxicity study of silver nanoparticles in Sprague-Dawley rats. Inhal Toxicol 2007;19(10):857–71.
[14] Kim YS, Kim JS, Cho HS, Rha DS, Kim JM. Twenty-eight-day oral toxicity, genotoxicity, and gender-related tissue distribution of silver nanoparticles in Sprague-Dawley rats. Inhal Toxicol 2008;20(6):575–83.
[15] Vlachou E, Chipp E, Shale E, Wilson YT, Papini R, Moiemen NS. The safety of nanocrystalline silver dressings on burns: a study of systemic silver absorption. Burns 2007;33(8):979–85.
[16] Wang XQ, Kempf M, Mott J, Chang HE, Francis R, Liu PY, et al. Silver absorption on burns after the application of Acticoat: data from pediatric patients and a porcine burn model. J Burn Care Res 2009;30(2):341–8.
[17] De Jong WH, Hagens WI, Krystek P, Burger MC, Sips AJAM, Geertsma RE. Particle size-dependent organ distribution of gold nanoparticles after intravenous administration. Biomaterials 2008;29(12):1912–9.
[18] Xie G, Sun J, Zhong G, Shi L, Zhang D. Biodistribution and toxicity of intravenously administered silica nanoparticles in mice. Arch Toxicol 2010;84(3):183–90.
[19] Brown RP, Delp MD, Lindstedt SL, Rhomberg LR, Beliles RP. Physiological parameter values for physiologically based pharmacokinetic models. Toxicol Ind Health 1997;13:407–84.
[20] Vaupel P, Ruppert H, Hutten H. Splenic blood flow and intrasplenic flow distribution in rats. Pflugers Arch 1977;369(3):193–201.
[21] Choi HS, Liu W, Misra P, Tanaka E, Zimmer JP, Ipe BI, et al. Renal clearance of quantum dots. Nat Biotechnol 2007;25(10):1165–70.
[22] Wang J, Zhou G, Chen C, Yu H, Wang T, Ma Y, et al. Acute toxicity and biodistribution of different sized titanium dioxide particles in mice after oral administration. Toxicol Lett 2007;168(2):176–85.
[23] Yang RSH, Chang LW, Wu J-P, Tsai M-H, Wang H-J, Kuo Y-C, et al. Persistent tissue kinetics and redistribution of nanoparticles, quantum dots 705, in mice: ICP-MS quantitative assessment. Environ Health Perspect 2007;115 (9):1339–43.
[24] Ma HL, Xu YF, Qi XR, Maitani Y, Nagai T. Superparamagnetic iron oxide nanoparticles stabilized by alginate: pharmacokinetics, tissue distribution, and applications in detecting liver cancers. Int J Pharm 2008;354 (1–2):217–26.
[25] Mikhail AS, Allen C. Block copolymer micelles for delivery of cancer therapy: transport at the whole body, tissue and cellular levels. J Control Release 2009;138(3):214–23.
[26] Balasubramanian SK, Jittiwat J, Manikandan J, Ong C-N, Yu LE, Ong W-Y. Biodistribution of gold nanoparticles and gene expression changes in the liver and spleen after intravenous administration in rats. Biomaterials 2010;31 (8):2034–42.
[27] Li SD, Huang L. Pharmacokinetics and biodistribution of nanoparticles. Mol Pharm 2008;5(4):496–504.
[28] Ehrenberg MS, Friedman AE, Finkelstein JN, Oberdörster G, McGrath JL. The influence of protein adsorption on nanoparticles association with cultured endothelial cells. Biomaterials 2009;30(4):603–10.
[29] Nel AE, Mädler L, Velegol D, Xia T, Hoek EM, Somasundaran P, et al. Understanding biophysicochemical interactions at the nano-bio interface. Nat Mater 2009;8(7):543–57.